

Examining F-actin interaction with intact talin and talin head and tail fragment using static and dynamic light scattering

Wolfgang H. GOLDMANN¹, Zeno GUTTENBERG¹, Stefan KAUFMANN², Daniel HESS², Robert M. EZZELL¹ and Gerhard ISENBERG²

¹ Department of Surgery, Surgery Research Laboratories, Massachusetts General Hospital, Harvard Medical School, Charlestown, USA

² Department of Biophysics, E22, Technical University of Munich, Garching, Germany

(Received 4 September 1997) – EJB 97 1270/4

We examined the binding kinetics of intact talin and talin head and tail fragment with F-actin at pH 7.0 and at low ionic strength. We observed by a transient kinetic method a fast followed by a slower binding process for intact talin and talin tail fragment with filamentous actin. The latter can be attributed to F-actin cross-linking and/or bundling, which was observed in cosedimentation assays as well as by low shear viscometry and electron microscopy [Zhang, J., Robson, R. M., Schmidt, J. M. & Stromer, M. H. (1996) *Biochem. Biophys. Res. Commun.* 218, 530–537]. This finding is supported by dynamic light scattering measurements, indicating changes in internal actin filament dynamics due to cross-linking/bundling events with intact talin and talin tail fragment. No binding of the talin head fragment with F-actin was detected by either method.

Keywords: talin; actin; stopped-flow kinetics; dynamic light scattering.

Talin is one link in the chain of cytoskeletal proteins that form a structure that functions both to detect and signal changes in the extracellular and intracellular milieu and to bring about cellular responses [1]. The transmembrane proteins mediating these contacts are members of a family of integrins. Integrins are heterodimeric complexes in which both chains span the plasma membrane bilayer once; the cytoplasmic domain of the β -chain is responsible for linkage to the actin cytoskeleton. A major protein component of focal adhesions is talin. Originally, it was thought that talin was linked to the actin filaments through other proteins such as vinculin [2–4] and α -actinin [5]. Talin has also been shown to bind directly to G-actin and F-actin [6–9], and recent studies with glutathione *S*-transferase (GST) fusion proteins indicate two non-overlapping F-actin-binding regions in the C-terminal and the possibility of another binding site in the N-terminal region [10]. Furthermore, talin binds to lipid bilayers, in several ways. A portion of the talin head can insert into charged phospholipids, connecting the actin cytoskeleton to the lipid membrane [11–14].

Mouse talin consists of 2541 amino acids and can be cleaved into an \approx 50-kDa head and an \approx 220-kDa tail region [15]. We and others have examined the molecule using electron microscopy and have found human platelet talin to be an antiparallel homodimer of 51 nm in length [16], and smooth muscle talin predominantly in a highly flexible, monomeric form [17]. These structural differences may be due to the protein source, protein concentrations, and buffer conditions used in these experiments. Recent observations by Zhang et al. [18] have shown that the talin molecule is sensitive to changes in pH and ionic strength, which allow it to cross-link actin to form filament bundles and networks. In the present study, we used static and dynamic light

scatter methods to examine the binding reaction of F-actin to intact talin as well as to talin head and tail fragment at pH 7.0 and low ionic strength.

MATERIALS AND METHODS

Protein preparation. Actin was prepared according to the procedure of Spudich and Watt [19] from acetone powder obtained from rabbit back muscle. The biological activity of the purified actin was tested using falling ball viscometry, and its concentration was determined using an absorption coefficient, ϵ_{290} , of $26\,460\text{ M}^{-1}\text{ cm}^{-1}$. G-actin was stored in G-buffer: 2 mM Tris/HCl, pH 7.5; 0.2 mM CaCl_2 , 0.5 mM ATP, 0.2 mM dithiothreitol and 0.005% NaN_3 , either kept on ice for less than two days or rapidly frozen using liquid nitrogen, kept at -80°C , and thawed immediately before use. For the light scattering studies, G-actin was polymerized overnight at 4°C in F-buffer containing 2 mM Tris/HCl, pH 7.5, 100 mM KCl, 2 mM MgCl_2 , 0.2 mM CaCl_2 , 0.2 mM dithiothreitol, 0.5 mM ATP.

Platelet talin was isolated from outdated human thrombocytes by the Collier and Wang method [20]. Talin was further purified by passing it through a gel filtration column [7]. Proteolytic cleavage of talin was achieved by thrombin digestion at room temperature [13]. The purities of the intact talin as well as talin head and tail fragment were analyzed on SDS/polyacrylamide gel, and protein concentration was determined according to the method of Bradford [21] (Fig. 1).

Stopped-flow experiments. The rapid mixing studies were performed at ambient temperature in a stopped flow spectrophotometer SF-61 (supplied by Hi-Tech Scientific Ltd, Salisbury, UK), as shown in Fig. 2. The dead time of the apparatus is \approx 2 ms. The optical system consists of a 100-W mercury lamp (Osram HBO 100W/2), with the monochromator set at 355 nm and a slit width of 2 nm. The light is transmitted via a light guide to the mixing/observation chamber, and the emitted light is monitored (at 90° to the incident light) by the photomultiplier.

Correspondence to W. H. Goldman, Massachusetts General Hospital, Harvard Medical School, Department of Medicine, Building 149, 13th Street, Charlestown, MA 02129, USA

Fax: +1 617 726 5669.

E-mail: goldman@helix.mgh.harvard.edu

Abbreviations. $k_{\text{obs}1}$ and $k_{\text{obs}2}$, observed rates.

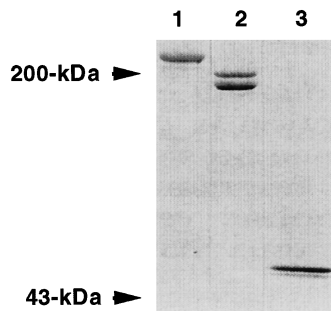


Fig. 1. 5–15% gradient SDS/polyacrylamide showing intact talin (lane 1), talin tail (lane 2), and talin head fragments (lane 3). Each lane was loaded with 2.5 μ g protein. The molecular masses are indicated on the left.

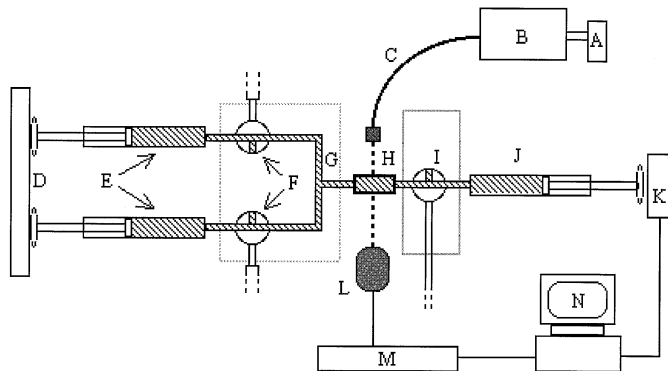


Fig. 2. Schematic diagram of the stopped-flow apparatus. (A) Light source, (B) monochromator, (C) light guide, (D) drive plate, (E) driving syringes, (F) reservoir syringes, (G) mixing chamber, (H) observation/reaction cell, (I) waste syringe, (J) stopping syringe, (K) stopping block, (L) photomultiplier, (M) acquisition system, and (N) computer.

The signal captured by the photomultiplier is electronically filtered by a unity gain amplifier. The time constant is normally set at 0.1% of the total sweep time. The voltage output from the photomultiplier is digitized by an analog converter before being transferred to a Macintosh computer IIfx and analyzed on a commercially available program (IGOR Pro 3).

Dynamic light scattering experiments. The dynamic light scatter studies were carried out in a device supplied by Brookhaven Instruments (Holtsville, NY, USA; Fig. 3). A spectral line at 633 nm from a 10-mW He-Ne laser, used as light source, is transmitted through the sample held in a glass tube of 8 mm inner diameter. The aperture prior to light entering the quartz cell and the photomultiplier are computer controlled to minimize stray light. The detected light is directly transmitted to the correlator and analyzed by computer.

RESULTS

Stopped-flow studies. The association rates were obtained by the stopped-flow method. F-actin was mixed with intact talin as well as talin head and tail fragment. The light scatter transients at 355 nm are best described by a double exponential as a single exponential did not fit the data adequately. Fig. 4 A and B show a typical result of six averaged light scatter signals of an F-actin and intact talin and talin tail solution with a least-squares exponential fit superimposed. The observed rates, k_{obs1} and k_{obs2} , with respect to 3 μ M F-actin and 2 μ M intact talin and talin tail fragment solution were 0.11 s^{-1} and 0.021 s^{-1} and 0.75 s^{-1} and

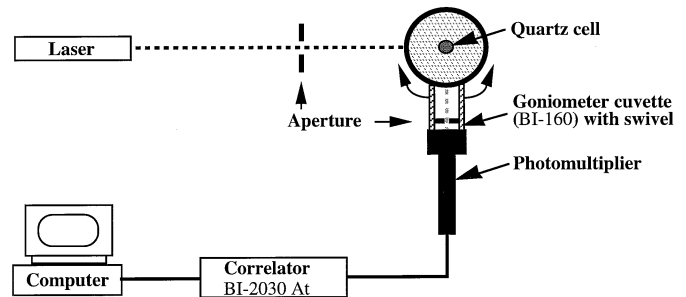


Fig. 3. Schematic representation of the dynamic light scatter apparatus consisting of a laser, quartz cell, goniometer cuvette with swivel, photomultiplier, correlator, and computer.

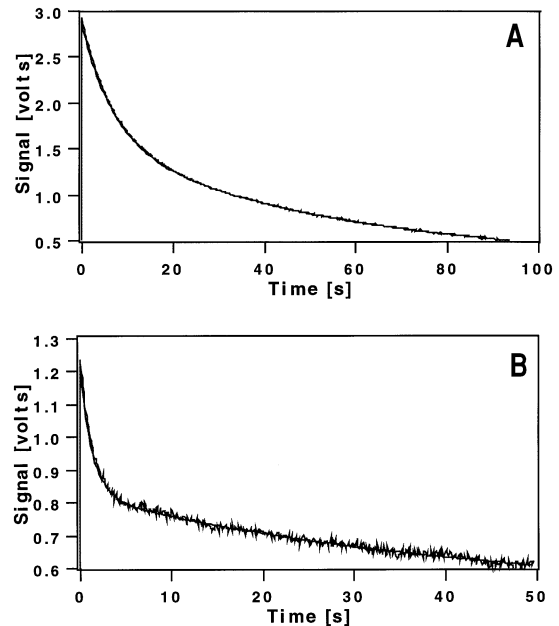


Fig. 4. Stopped-flow analysis. The traces represent the average of six consecutive measurements in the stopped-flow apparatus. Changes in light scattering signal at a 90° angle and 355 nm wavelength were detected at 2 μ M intact talin (A) and 2 μ M talin tail fragment (B) with 3 μ M F-actin (cell reaction concentration). Conditions were as follows: temperature, 20°C; buffer, 20 mM Tris/HCl, pH 7.0, 1 mM EGTA, 1 mM dithiothreitol. The best-fit line to the data give values of 0.11 s^{-1} and 0.021 s^{-1} (A) and 0.75 s^{-1} and 0.024 s^{-1} (B), respectively. The values presented correspond to the observed rates, k_{obs1} and k_{obs2} .

0.024 s^{-1} , respectively. The difference between the first and second rate is significant and indicates that probably two events are occurring: a faster binding process and a slower actin cross-linking/bundling reaction. This result follows a trend observed by Zhang et al. [18] that pH less than 7.4 and low ionic strength regulate the binding of intact talin and probably talin tail fragment to actin, bringing about the stabilization of actin filaments. Control experiments using F-actin and talin head fragment under identical conditions showed no significant signal change above the noise level. This confirms earlier findings by Niggli et al. [13] and Mugeruma et al. [22] that this fragment is probably not involved in actin binding, but is contrary to the predictions of Hemmings et al. [10] of a possible actin-binding site in the head region (data not shown).

Dynamic light scattering studies. We measured the autocorrelation function which gives information about the internal polymer dynamics of the scattered light intensity of actin filaments

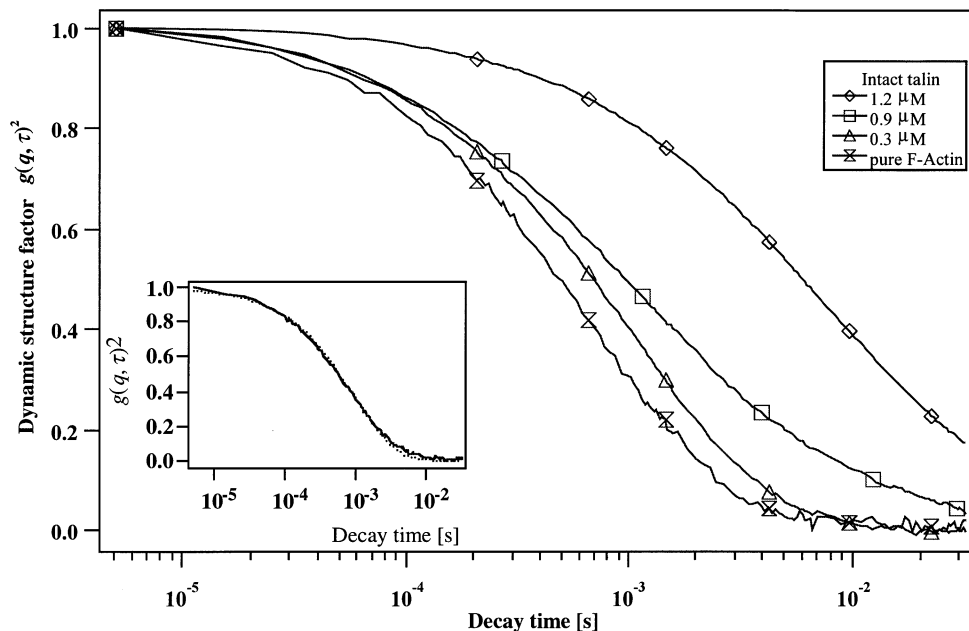


Fig. 5. Plot of the dynamic structure factor $g(q, \tau)^2$ against decay times (between 5×10^{-5} and 5×10^{-1} s) of $3 \mu\text{M}$ F-actin in the absence and presence of 0.3 , 0.9 , and $1.2 \mu\text{M}$ intact talin. Conditions were as follows: temperature, 22°C ; measuring time, 10 min; wavelength, 633 nm; buffer as described in the legend of Fig. 4. The inset depicts a light dynamic light scatter trace of $3 \mu\text{M}$ F-actin with the best fit superimposed (\cdots), using the autocorrection function $g(q, \tau) = (-b\tau^{0.75})$; $b = 106.4$; residuals $< 5\%$. b is a constant, q is the scattering vector and τ is the correlation time. (Note: for further reading and general structure predictions cf. [28].)

in the presence of intact talin as well as talin head and tail fragment. The theoretical approach described by Goetter et al. [23] allowed a good approximation of the dynamics of semiflexible polymers within a time range of 10^{-5} – 10^{-2} s.

Prior to experimentation, we measured pure F-actin solutions. Normalizing the amplitude to a value of one, the data were fitted over the entire time range and the dependency at a 90° angle followed a q^2 -law (see inset to Fig. 5, dotted line). To investigate the scattering behavior of F-actin solutions in the presence of intact talin as well as talin head and tail fragment, we incubated the proteins at various concentrations. Fig. 5 shows the results from experiments with intact talin and F-actin, where we plot the amplitudes $g(q, \tau)^2$ against decay times at a scattering angle of 90° . Increasing the talin protein concentration indicates a decrease in amplitude and a change in curve structure over time. Fitting the function to the data, we determined the constant b . With increasing intact talin and talin tail fragment concentrations, there is a slowing down of the decay, which is properly due to cross-linking and the formation of actin bundles (Table 1). Thus, no change occurred in the presence of the talin head fragment at increasing concentrations, indicating that only the association of intact talin and talin tail fragment with F-actin change the internal dynamic behavior of actin filaments.

DISCUSSION

In the present study, we examined the binding parameters of intact human platelet talin as well as talin head and tail fragment with F-actin using static light scattering, and we confirmed these observations using dynamic light scattering. Previously, Zhang et al. [18] have shown using cosedimentation, low shear viscometry, and electron microscopy that smooth muscle talin is a potential cross-linking protein with F-actin. In their study, these researchers observed a specific interaction of actin with intact talin that was strongly dependent on the pH and ionic strength of the solution.

Table 1. The calculated values b for $3 \mu\text{M}$ F-actin in the absence and presence of intact talin as well as talin head and tail fragment at various concentrations.

Protein concentration	$g(q, \tau) = (-b\tau^{0.75})$ (b)		
	intact talin	talin tail fragment	talin head fragment
μM			
0 (pure F-actin)	106.4	106.4	106.4
0.3	89.6		
0.4		90.2	105.0
0.9	95.0		
1.2	44.5	53.2	104.4

We were interested to evaluate the binding events under these conditions using transient kinetic methods. Measuring association rates k_{obs1} and k_{obs2} of F-actin solutions with intact talin and talin tail fragment, we observed two significantly different binding reactions. The distinct relaxations could be described as a fast binding event followed by a slower process. These results confirm (a) reports by Hemmings et al. [10] of two actin-binding sites on the talin tail fragment, and (b) observations by Zhang et al. [18] of actin filament cross-linking at pH less than 7.4 and low ionic strength in the presence of intact talin. The kinetic events described here can be attributed specifically to an initial binding event followed by a cross-linking/bundling process. Support for this notion comes also from our dynamic light scatter data, where we noticed a correlation between rising (intact and tail fragment) talin concentration and increasing actin filament stiffness. The difference in the first binding rate of F-actin to intact talin and ≈ 220 -kDa tail fragment may be due to structural differences in the molecules.

Recently, Winkler et al. [17] have used energy-filtered electron microscopy to unravel the structural properties of smooth muscle talin. These researchers found this protein highly elongated, flexible, and mainly in monomeric form, which would allow the formation of a variety of molecular shapes and conformations. Previously, Zhang et al. [18] reported a regulatory effect of pH and ionic strength on the ability of talin molecules to cross-link filamentous actin and induce bundle and network formation. These parameters have a strong influence on the viscosity of actin-talin solutions, which has also been observed by McCann and Craig [24] using electron microscopy.

In earlier studies applying falling ball viscometry, rheology, and light microscopy, we showed that human platelet talin has an effect on the viscoelastic properties of actin filaments and on the internal dynamics of actin filaments, even at pH 7.5–8.0 and at ≈ 120 mM ionic strength. Using electron microscopy under these conditions, we observed no cross-linking, leading us to believe at that time that the talin molecule probably binds laterally to actin filaments [8, 25, 26].

More recently, using magnetometry and atomic force microscopy, we examined the influence of talin in focal adhesion complexes on F9 embryonic carcinoma cells. The absence of the talin-binding site on vinculin reduced the stiffness and viscosity of the entire cell by $\approx 20\%$ and had a significant influence on the ability of the cell to spread, adhere, and move [27]. These and our new results support the notion that talin (a) plays a key role as a mechanical molecular bridge in focal adhesions, (b) guides proper adhesion site formation, and (c) influences the integrin-mediated locomotion and viscoelasticity of the cell.

We are grateful to Dr Jay X. Tang (Harvard Medical School) for assisting us with the dynamic light scattering measurements. We would also like to thank Ms Judith Feldmann and Ms Elizabeth Nicholson for proofreading this manuscript and Klaus Kroy (Technical University of Munich) for his valuable comments. This work was supported by the *Deutsche Forschungsgemeinschaft*, the American Cancer Society, and the North Atlantic Treaty Organisation.

REFERENCES

- Isenberg, G. (1996) New concepts for signal perception and transduction by the actin cytoskeleton at cell boundaries, *Sem. Cell Dev. Biol.* 7, 707–715.
- Otto, J. J. (1983) Detection of vinculin-binding proteins with an ^{125}I -vinculin gel overlay technique, *J. Cell Biol.* 97, 1283–1287.
- Burridge, K. & Mangeat, P. (1984) An interaction between vinculin and talin, *Nature* 308, 744–746.
- Nuckolls, G. H., Turner, C. E. & Burridge, K. (1990) Functional studies of the domains of talin, *J. Cell Biol.* 110, 1635–1644.
- Muguruma, M., Matsumura, S. & Fukazawa, T. (1992) Augmentation of α -actinin-induced gelation of actin by talin, *J. Biol. Chem.* 267, 5621–5624.
- Muguruma, M., Matsumura, S. & Fukazawa, T. (1990) Direct interactions between talin and actin, *Biochem. Biophys. Res. Commun.* 171, 1217–1223.
- Kaufmann, S., Piekenbrock, T., Goldmann, W. H., Baermann, M. & Isenberg, G. (1991) Talin binds to actin and promotes filament nucleation, *FEBS Lett.* 284, 187–191.
- Goldmann, W. H. & Isenberg, G. (1991) Kinetic determination of talin-actin binding, *Biochem. Biophys. Res. Commun.* 178, 718–723.
- Schmidt, J. M., Robson, R. M., Zhang, J. & Stromer, M. H. (1993) The marked pH dependence of the talin-actin interaction, *Biochem. Biophys. Res. Commun.* 197, 660–666.
- Hemmings, L., Rees, D. J. G., Ohanian, V., Bolton, S. J., Gilmore, A. P., Patel, B., Priddle, H., Trevithick, J. E., Hynes, R. O. & Critchley, D. R. (1996) Talin contains three actin-binding sites each of which is adjacent to a vinculin binding site, *J. Cell Sci.* 109, 2715–2726.
- Goldmann, W. H., Niggli, V., Kaufmann, S. & Isenberg, G. (1992) Probing actin and liposome interaction of talin and talin-vinculin complexes: a kinetic, thermodynamic and lipid labeling study, *Biochemistry* 31, 7665–7671.
- Kaufmann, S., Kaes, J., Goldmann, W. H., Sackmann, E. & Isenberg, G. (1992) Talin anchors and nucleates actin filaments at lipid membranes: a direct demonstration, *FEBS Lett.* 314, 203–205.
- Niggli, V., Kaufmann, S., Goldmann, W. H., Weber, T. & Isenberg, G. (1994) Identification of functional domains in the cytoskeletal protein talin, *Eur. J. Biochem.* 224, 951–957.
- Tempel, M., Goldmann, W. H., Isenberg, G. & Sackmann, E. (1995) Interaction of the 47-kDa talin fragment and the 32-kDa vinculin fragment with acidic phospholipids: a computer analysis, *Biophys. J.* 69, 228–241.
- Rees, D. J. G., Ades, S. E., Singer, S. J. & Hynes, R. O. (1990) Sequence and domain structure of talin, *Nature* 347, 685–689.
- Goldmann, W. H., Bremer, A., Haener, M., Aebi, U. & Isenberg, G. (1994) Native talin is a dumbbell-shaped homodimer when it interacts with actin, *J. Struct. Biol.* 112, 3–10.
- Winkler, J., Luensdorf, H. & Jockusch, B. M. (1997) Energy-filtered electron microscopy reveals that talin is a highly flexible protein composed of a series of globular domains, *Eur. J. Biochem.* 243, 430–436.
- Zhang, J., Robson, R. M., Schmidt, J. M. & Stromer, M. H. (1996) Talin can crosslink filaments into both networks and bundles, *Biochem. Biophys. Res. Commun.* 218, 530–537.
- Spudich, J. A. & Watt, S. (1971) The regulation of rabbit skeletal muscle contraction. I. Biochemical studies of the interaction of the tropomyosin-troponin complex with actin and the proteolytic fragments of myosin, *J. Biol. Chem.* 246, 4866–4871.
- Collier, N. C. & Wang, K. (1982) Human platelet p235: a high M_r protein which restricts the length of actin filaments, *FEBS Lett.* 143, 205–210.
- Bradford, M. M. (1976) A rapid and sensitive method for the quantitation of microgram quantities of protein utilizing the principle of protein-dye binding, *Anal. Biochem.* 72, 248–254.
- Muguruma, M., Nishimuta, S., Tomisaka, Y., Ito, T. & Matsumura, S. (1995) Organization of the functional domains in membrane cytoskeletal protein talin, *J. Biochem. (Tokyo)* 117, 1036–1042.
- Goetter, R., Kroy, K., Frey, E., Baermann, M. & Sackmann, E. (1995) Dynamic light scattering from semidilute actin solutions: a study of hydrodynamic screening, filament bending stiffness, and the effect of tropomyosin/troponin-binding, *Macromolecules* 29, 30–36.
- McCann, R. O. & Craig, S. W. (1997) The I/LWEQ module: a conserved sequence that signifies F-actin binding in functionally diverse proteins from yeast to mammals, *Proc. Natl Acad. Sci. USA* 94, 5679–5684.
- Ruddies, R., Goldmann, W. H., Isenberg, G. & Sackmann, E. (1993) The viscoelasticity of entangled networks: the influence of defects and the modulation by talin and vinculin, *Eur. Biophys. J.* 22, 309–321.
- Goldmann, W. H., Kaes, J. & Isenberg, G. (1993) Talin decreases the bending elasticity of actin filaments, *Biochem. Soc. Trans.* 22, 46S.
- Galneder, R., Ludwig, M., Goldmann, W. H., Wang, N., Gaub, H. E. & Ezzell, R. M. (1996) Differences in viscoelasticity of vinculin-deficient F9 cells measured by magnetometry and atomic force microscopy, *Mol. Biol. Cell* 7, 385a.
- Kvoy, K. & Frey, E. (1997) Dynamic scattering from solutions of semiflexible polymers, *Physical Review E* 55, 3092–3101.